Article

TiO$_2$ Nano Flowers Based EGFET Sensor for pH Sensing

Chih-Chiang Yang [1,*] ![ORCID], **Kuan-Yu Chen [1,2]** ![ORCID] **and Yan-Kuin Su [1,2,3,*]**

[1] Green Energy Technology Research Center, Kun Shan University, Tainan 710, Taiwan; cncer7025@gmail.com
[2] Department of Electrical Engineering, Institute of Microelectronics, National Cheng Kung University, Tainan 701, Taiwan
[3] Department of Electrical Engineering, Kun Shan University, Tainan 710, Taiwan
*   Correspondence: 298r.yang@gmail.com (C.-C.Y.); yksu@mail.ncku.edu.tw (Y.-K.S.); Tel.: +886-6-275-7575 (ext. 62400-1216) (C.-C.Y.); +886-6-275-7575 (ext. 62382) (Y.-K.S.)

check for updates

Abstract: In this study, pH sensors were successfully fabricated on a fluorine-doped tin oxide substrate and grown via hydrothermal methods for 8 h for pH sensing characteristics. The morphology was obtained by high-resolution scanning electron microscopy and showed randomly oriented flower-like nanostructures. The TiO$_2$ nanoflower pH sensors were measured over a pH range of 2–12. Results showed a high sensitivity of the TiO$_2$ nano-flowers pH sensor, 2.7 $(\mu A)^{1/2}$/pH, and a linear relationship between I$_{DS}$ and pH (regression of 0.9991). The relationship between voltage reference and pH displayed a sensitivity of a 46 mV/pH and a linear regression of 0.9989. The experimental result indicated that a flower-like TiO$_2$ nanostructure extended gate field effect transistor (EGFET) pH sensor effectively detected the pH value.

Keywords: EGFET; TiO$_2$; hydrothermal synthesis

1. Introduction

The pH value, which is defined as the negative logarithm of hydrogen ion concentration, is a standardized scale for determining whether a solution is alkaline or acidic. The more acidic is the liquid, the greater the amount of hydrogen ions. Acid–base sensing has been used in numerous applications, such as water quality testing, food safety, agriculture, chemistry, and medical care, indicating its importance [1–3].

To date, pH sensors that are the most commonly used are pH test strips and meters. A pH test strip is a simple, low cost, and fast method, but its disadvantage is that the specific pH value cannot be accurately determined. On the contrary, a pH meter commonly uses glass electrodes, which are costly and fragile, proving difficult to maintain. On this basis, two types of typical sensing components are available. One is the ion-sensitive field-effect transistor (ISFET), and the other is the extended gate field effect transistor (EGFET) [4,5], which are used to measure the hydrogen ion concentration in the medium. ISFET is similar to the metal-oxide-semiconductor field-effect transistor (MOSFET). The difference is that the metal gate of the MOSFET is changed to an insulating layer (e.g., SiO$_2$) as a sensing layer. To determine the pH value, the concentration of hydrogen ions, which change the surface potential and the transistor's current, is identified. Different from ISFET, EGFET has an independent layer structure fabricated on the end of the signal line extended from the field-effect transistor gate electrode. The independent layer mostly uses metal oxide as a sensing membrane, which can attract the hydrogen ions in the solution. In comparison with ISFET, EGFET has several advantages: (1) the sensing region is separated from the gate-controlled region, which simply replaces the sensing film, so it can be developed as a disposable component; (2) it is easy to package due to
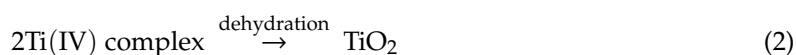
its relatively simple structure; (3) the sensing film can be easily switched; and (4) there is no light interference [5].

Metal oxides, such as ZnO, CuO, SnO_2, and WO_3 have been widely used as sensing films in numerous studies [6–9]. TiO_2 is a semiconductor, which has received considerable attention due to its superior chemical stability, including nontoxicity, acid and alkaline resistance, low cost, and is easy to process [10]. Accordingly, TiO_2 has been utilized in gas sensors, UV photodetectors, memory resistors, and water treatment cleaning applications [11–17]. By contrast, the thin film-based sensing membrane has poor sensitivity. On the basis of the poor sensitivity, several studies have reported a nanostructure, which can enhance the component performance due to the large surface area [18]. The nanostructure can be fabricated by self-assembly growth processes, such as the hydrothermal method and sputtered and metal organic chemical vapor deposition (CVD). However, sputter and CVD methods should be used under a high-vacuum ambient environment. In addition, their source materials are expensive. Thus, the hydrothermal method is mostly used because of its advantages, such as low-cost fabrication, low-temperature process, and easy processing [19].

In this work, to increase the device sensitivity, we prepared a TiO_2 nanostructure on a fluorine-doped tin oxide (FTO) substrate via the hydrothermal method. The TiO_2 EGFET pH sensor was measured with a solution of pH 2–12. The device performance and the material analysis are also discussed herein.

2. Experiment

For the device preparation, $2 \times 2 \, cm^2$ FTO glass was cleaned by acetone, isopropanol, and deionized (DI) water using an ultrasonicator (DELTA D150, Taipei, Taiwan). The FTO substrate that can be prepared in a strong acid environment also has small lattice mismatch with TiO_2 [20]. Before cleaning, the 0.5 cm fluoroplastic adhesive tape sticks (Nitto Denko No.903UL, Osaka, Japan) were placed on the substrate and used as an electrode. Figure 1 shows the schematic diagram of the TiO_2 EGFET pH sensor. The precursor solution was premixed with DI water (30 mL) and 36% hydrochloric acid (30 mL), added with titanium(IV) *n*-butoxide (>99%, 2 mL), and ultrasonicated for 20 min. The formation reaction of TiO_2 is shown in the following equation [21]:

$$TiCl_4 + H_2O \rightarrow HCl + Ti(IV) \text{ complex} \tag{1}$$

$$2Ti(IV) \text{ complex} \xrightarrow{\text{dehydration}} TiO_2 \tag{2}$$

After completing the preparation, the precursor was placed in a Teflon autoclave, and the sample was positioned facing upward. Then, the Teflon autoclave was placed in a hot oven and heated at 150 °C for 8 h. Finally, the sample underwent argon flow annealing for 60 min at 300 °C. A standard buffer solution (Great & Best Co., Ltd., Taipei, Taiwan) was used in the sensing measurement at a range of pH 2–12. Characterization of the TiO_2 nanostructure included X-ray diffraction (XRD, D8 Discover, Bruker, Billerica, MA, USA), high-resolution scanning electron microscopy (HR-SEM, HITACHI SU8000, Tokyo, Japan), and energy-dispersive spectroscopy (EDS), as discussed further below. Semiconductor parameter analyzer 4145B (Keysight Technologies, Santa Rosa, CA, USA) was set up to measure the current–voltage (*I*–*V*) characteristic curves. The pH sensing electrode was connected to the gate (pin 6) of a commercial CD4007UB *n*-type MOSFET, and pins 7 and 8 corresponded to the source and drain, respectively. A commercial Ag/AgCl electrode was used as reference electrode. The distance between the reference and sensing electrodes was fixed at approximately 2 cm, and the process was performed in a dark room at room temperature. Figure 2 shows the schematic diagram of the measuring device.
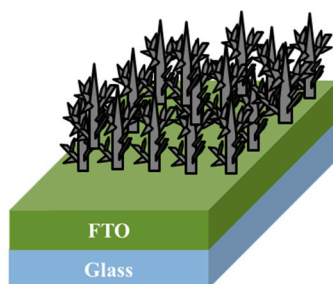
Figure 1. Schematic diagram of the TiO_2 extended gate field effect transistor (EGFET) sensor.
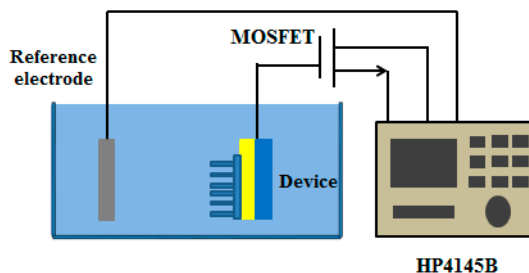

Figure 2. EGFET measurement system.

3. Results and Discussion

Figure 3 shows the XRD pattern of synthesized TiO_2 nanoflowers and the peaks at $2\theta = 27.46°$, 36.11°, 41.26°, 44.08°, 54.37°, 56.69°, 62.79°, 64.09°, 69.07°, and 69.85°, which correspond to (110), (101), (111), (210), (211), (220), (002), (310), (301), and (112) planes, respectively, indicating that the sample of TiO_2 nanoflower was tetragonal rutile TiO_2, which can be indexed to JCPDS card no. 21-1276. Figure 4 shows the top view of the HR-SEM image of the hydrothermal synthesis of TiO_2 samples, revealing a crystalline flower-like and randomly oriented structure. Meanwhile, the EDS analyses detected only Ti and oxygen. The atomic percentages of Ti and oxygen were 43.28 at.% and 56.72 at.%, respectively, and no other elements were detected (insert in Figure 3).
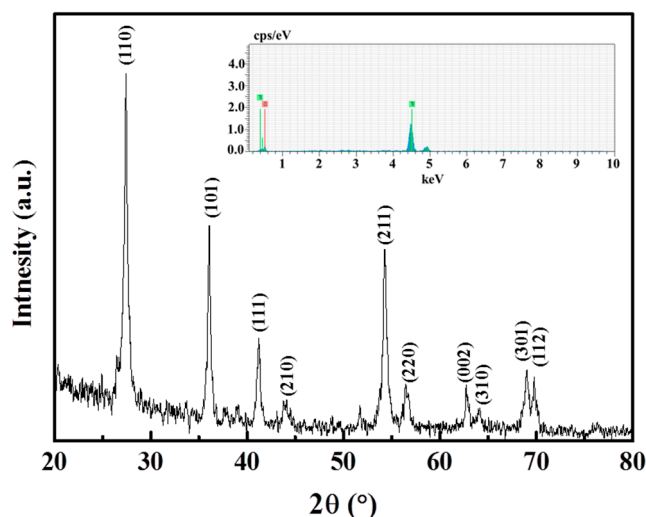
Figure 3. XRD pattern of synthesized TiO_2 nano-flowers.

(a)　　　　　　　　　　　　　　　　　　　**(b)**
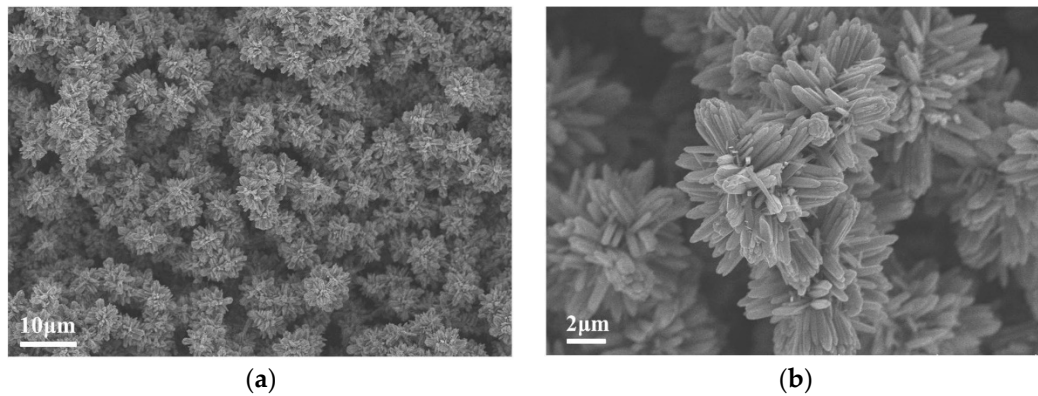
Figure 4. (**a**) Top view of HR-SEM image of synthesized TiO$_2$ nano-flowers, which show the randomly oriented flower-like nanostructures. (**b**) The high-magnified HR-SEM image of TiO$_2$ nano-flowers.

Figure 5a shows the V_{ref}-I_{DS} transfer characteristic of the device, setting the MOSFET at a gate voltage of 0–3 V and at V_{DS} = 0.3 V in pH 2–12 buffer solution. V_{ref} decreased with an increase in the pH value due to the lower H$^+$ ion concentrations in the buffer solution, decreasing the surface potential of the sensing electrode. $V_{T(EGFET)}$ can be expressed as follows [22]:

$$V_{T(EGFET)} = V_{T(MOSFET)} - \frac{\varnothing_M}{q} + E_{ref} + X^{Sol} - \varphi \qquad (3)$$

where $V_{T(MOSFET)}$ is the threshold voltage of MOSFET, $\varnothing_M$ denotes the work function of the reference electrode, q represents the electron charge, E_{ref} indicates the potential of the reference electrode, X^{Sol} refers to the surface dipole potential of the buffer solution, and φ signifies the surface potential at the electrolyte/sensing film interface. Figure 5b shows the V_{ref} value as a function of pH value. The pH sensitivity from the liner pH-V_{ref} can be expressed as follows:

$$sensitivity = \frac{\Delta V_T}{\Delta pH} \qquad (4)$$

The V_{ref} values were 1.53, 1.66, 1.74, 1.84, 1.94, and 2 V for different pH values ranging from 2 to 12. The device sensitivity was 46 mV/pH and the high linear regression was 0.9989. Figure 6 shows the I_{DS}-V_{DS} output characteristic. The output characteristic of the device can be expressed as follows [23]:

$$I_{DS} = \frac{W\mu_n C_{ox}}{2L}\left[(V_{ref} - V_T)^2\right] \qquad (5)$$

where W and L are the channel width and length, respectively, C_{ox} repesents the oxide capacitance per unit area, μ_n denotes the electron mobility in the channel, and V_T indicates the threshold voltage. I_{DS} increased with the pH value from 12 to 2, indicating that the device can be modulated by various pH values. Figure 6b shows the I_{DS} value as a function of pH value. The pH current sensitivity from the linear pH-I_{DS} can be expressed as follows:

$$sensitivity = \frac{\Delta \sqrt{I_{DS}}}{\Delta pH} \qquad (6)$$

The I_{DS} values were 1.25, 1.19, 1.14, 1.08, 1.03, and 0.99 for different pH values ranging from 2 to 12. The current sensitivity of the device was 2.7 (μA)$^{1/2}$/pH, and the high linear regression was 0.9982. The sensing performance can be explained based on the site-binding model [24]. The surface potential depends on the pH of a buffer solution; thus, the sensing Ti-membrane has three different forms: negative (Ti-O$^-$), positive (Ti-OH^{2+}), and neutral (Ti OH). Furthermore, a lower pH value indicates a greater concentration of H$^+$ in the solution. Consequently, a high amount of H$^+$ is adsorbed onto

the sensing membrane. Table 1 displays the device sensitivity compared with other studies given the great specific surface area, resistance to high temperature, acid, and alkali, and high electrical conductivity of TiO_2 nanoflowers; as such, the device exhibited more potential than other EGFET pH sensors. Dar et al. [25] reported that glucose is easily oxidized by dynamic oxygen species, and metal oxide layers facilitate the release of trapped electrons back to the conduction band of metal oxide. Oxygen is absorbed at the interface of metal oxide, ionized, and converted into dynamic oxygen species. Chen et al. [26] reported that uric acid (UA) can be easily oxidized in common electrodes in aqueous solutions, thereby modifying the detection potential for different concentrations. Hence, these sensors have promising prospects for detection.
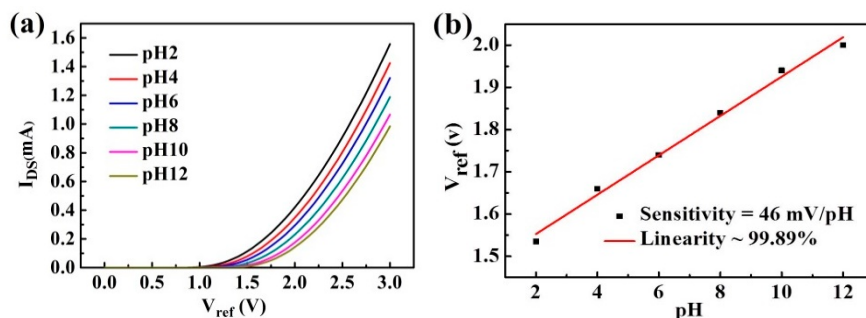
Figure 5. (**a**) I_{DS}-versus-V_{ref} curve under various pH buffer solutions. (**b**) Linearity of the V_{ref} of TiO_2 EGFET sensor.
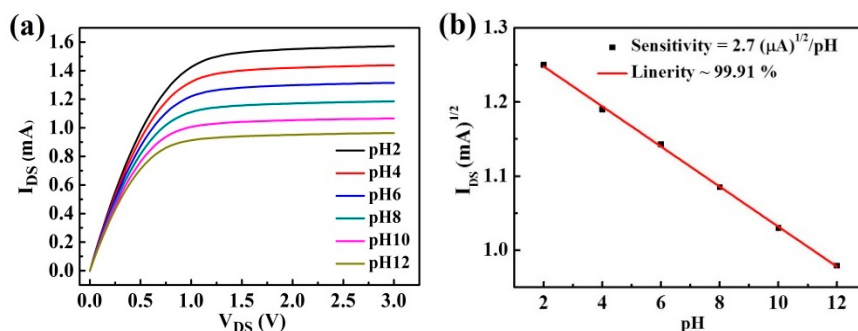
Figure 6. (**a**) I_{DS}-versus-V_{DS} curve under various pH buffer solutions. (**b**) Linearity of the I_{DS} of TiO_2 EGFET sensor.

Table 1. Comparison of other metal oxide-based extended gate field effect transistor (EGFET) pH sensors.

Sample	Fabrication Method	Sensitivity (mV/pH)	Ref.
ZnO thin film	sol–gel	26.5	[27]
V_2O_5/had	Hydrothermal	38.1	[28]
Porous TiO_2	Hydrothermal	19.3	[29]
TiO_2 nanowires	E-beam evaporator	32.65	[30]
TiO_2 nanoflower	Hydrothermal	46	This work

4. Conclusions

In this study, pH sensors were successfully fabricated on FTO substrate and grown via hydrothermal methods at 8 h for pH sensing characteristics. Results indicated that a pH sensor with a TiO_2 nanoflower can measure in the pH range of 2–12 buffer solution and the nanoflower growth has the best sensitivity and linear regression relationship between I_{DS} and pH, at 2.7 $(\mu A)^{1/2}$/pH and 0.9991, respectively. Moreover, the relationship among voltage reference, pH, and sensitivity was 46 mV/pH,

and the linear regression was 0.9989. Thus, this new approach is not only expected to be useful for pH sensors but also to detect glucose or uric acid via an advanced multifunctional biosensor.

References

1. Wang, Y.; Huang, T.; Liu, J.; Lin, Z.; Li, S.; Wang, R.; Ge, Y. Soil pH value, organic matter and macronutrients contents prediction using optical diffuse reflectance spectroscopy. *Comput. Electron. Agric.* **2015**, *111*, 69–77. [CrossRef]

2. Honma, T.; Ohba, H.; Kaneko-Kadokura, A.; Makino, T.; Nakamura, K.; Katou, H. Optimal soil Eh, pH, and water management for simultaneously minimizing arsenic and cadmium concentrations in rice grains. *Environ. Sci. Technol.* **2016**, *50*, 4178–4185. [CrossRef] [PubMed]

3. Schumacher, S.P.; Schurgers, L.J.; Vervloet, M.G.; Neradova, A. Influence of pH and phosphate concentration on the phosphate binding capacity of five contemporary binders. An in vitro study. *Nephrology* **2019**, *24*, 221–226. [CrossRef] [PubMed]

4. Moser, N.; Lande, T.S.; Toumazou, C.; Georgiou, P. ISFETs in CMOS and emergent trends in instrumentation: A review. *IEEE Sens. J.* **2016**, *16*, 6496–6514. [CrossRef]

5. Pullano, S.; Critello, C.; Mahbub, I.; Tasneem, N.; Shamsir, S.; Islam, S.; Greco, M.; Fiorillo, A.S. EGFET-based sensors for bioanalytical applications: A review. *Sensors* **2018**, *18*, 4042. [CrossRef]

6. Qi, J.; Zhang, H.; Ji, Z.; Xu, M.; Zhang, Y. ZnO nano-array-based EGFET biosensor for glucose detection. *Appl. Phys. A* **2015**, *119*, 807–811. [CrossRef]

7. Chen, P.Y.; Yin, L.T.; Cho, T.H. Optical and impedance characteristics of EGFET based on SnO_2/ITO sensing gate. *Life Sci. J.* **2014**, *11*, 871–875.

8. Guidelli, E.J.; Guerra, E.M.; Mulato, M. V_2O_5/WO_3 mixed oxide films as pH-EGFET sensor: Sequential re-usage and fabrication volume analysis. *ECS J. Solid State Sci. Technol.* **2012**, *1*, N39–N44. [CrossRef]

9. Chang, S.P.; Yang, T.H. Sensing performance of EGFET pH sensors with CuO nanowires fabricated on glass substrate. *Int. J. Electrochem. Sci.* **2012**, *7*, 5020–5027.

10. Galiano, F.; Song, X.; Marino, T.; Boerrigter, M.; Saoncella, O.; Simone, S.; Faccini, M.; Chaumette, C.; Drioli, E.; Figoli, A. Novel photocatalytic PVDF/nano-TiO_2 hollow fibers for environmental remediation. *Polymers* **2018**, *10*, 1134. [CrossRef]

11. Galstyan, V. Porous TiO_2-based gas sensors for cyber chemical systems to provide security and medical diagnosis. *Sensors* **2017**, *17*, 2947. [CrossRef]

12. Liu, H.Y.; Sun, W.C.; Wei, S.Y.; Yu, S.M. Characterization of TiO_2-based MISIM ultraviolet photodetectors by ultrasonic spray pyrolysis. *IEEE Photonics Technol. Lett.* **2016**, *28*, 637–640. [CrossRef]

13. Chen, Y.; Li, L.; Yin, X.; Yerramilli, A.; Shen, Y.; Song, Y.; Bian, W.; Li, N.; Zhao, Z.; Qu, W.; et al. Resistive switching characteristics of flexible TiO_2 thin film fabricated by deep ultraviolet photochemical solution method. *IEEE Electron Device Lett.* **2017**, *38*, 1528–1531. [CrossRef]

14. Lazar, M.; Varghese, S.; Nair, S. Photocatalytic water treatment by titanium dioxide: Recent updates. *Catalysts* **2012**, *2*, 572–601. [CrossRef]

15. Joshi, N.; Hayasaka, T.; Liu, Y.; Liu, H.; Oliveira, O.N., Jr.; Lin, L. A review on chemiresistive room temperature gas sensors based on metal oxide nanostructures, graphene and 2D transition metal dichalcogenides. *Mikrochim. Acta* **2018**, *185*, 213. [CrossRef] [PubMed]

16. Liu, X.; Ma, T.; Pinna, N.; Zhang, J. Two-dimensional nanostructured materials for gas sensing. *Adv. Funct. Mater.* **2017**, *27*, 1702168. [CrossRef]

17.　Zhang, J.; Liu, X.; Neri, G.; Pinna, N. Nanostructured materials for room-temperature gas sensors. *Adv. Mater.* **2016**, *28*, 795–831. [CrossRef] [PubMed]

18.　Zhang, Q.; Liu, W.; Sun, C.; Zhang, H.; Pang, W.; Zhang, D.; Duan, X. On-chip surface modified nanostructured ZnO as functional pH sensors. *Nanotechnology* **2015**, *26*, 355202. [CrossRef] [PubMed]

19.　Zhang, J.; Li, J.; Chen, P.; Rehman, F.; Jiang, Y.; Cao, M.; Zhao, Y.; Jin, H. Hydrothermal growth of VO_2 nanoplate thermochromic films on glass with high visible transmittance. *Sci. Rep.* **2016**, *6*, 27898. [CrossRef]

20.　Issar, S.; Poddar, P.; Mehra, N.C.; Mahapatro, A.K. Growth of flower-like patterns of TiO_2 nanorods over FTO substrate. *Integr. Ferroelectr.* **2017**, *184*, 166–171. [CrossRef]

21.　Kumar, A.; Madaria, A.R.; Zhou, C. Growth of aligned single-crystalline rutile TiO_2 nanowires on arbitrary substrates and their application in dye-sensitized solar cells. *J. Phys. Chem. C* **2010**, *114*, 7787–7792. [CrossRef]

22.　Das, A.; Ko, D.H.; Chen, C.H.; Chang, L.B.; Lai, C.S.; Chu, F.C.; Chow, L.; Lin, R.M. Highly sensitive palladium oxide thin film extended gate FETs as pH sensor. *Sens. Actuators B* **2014**, *205*, 199–205. [CrossRef]

23.　Bergveld, P. The impact of MOSFET-based sensors. *Sens. Actuators* **1985**, *8*, 109–127. [CrossRef]

24.　Yusof, K.A.; Abdul Rahman, R.; Zulkefle, M.A.; Herman, S.H.; Abdullah, W.F.H. EGFET pH sensor performance dependence on sputtered TiO_2 sensing membrane deposition temperature. *J. Sens.* **2016**, *2016*, 7594531. [CrossRef]

25.　Dar, G.N.; Umar, A.; Zaidi, S.A.; Baskoutas, S.; Kim, S.H.; Abaker, M.; Al-Hajry, A.; Al-Sayari, S.A. Fabrication of highly sensitive non-enzymatic glucose biosensor based on ZnO nanorods. *Sci. Adv. Mater.* **2011**, *3*, 901–906. [CrossRef]

26.　Chen, X.; Wu, G.; Cai, Z.; Oyama, M.; Chen, X. Advances in enzyme-free electrochemical sensors for hydrogen peroxide, glucose, and uric acid. *Microchim. Acta* **2013**, *181*, 689–705. [CrossRef]

27.　Ali, G.M. Interdigitated extended gate field effect transistor without reference electrode. *J. Electron. Mater.* **2017**, *46*, 713–717. [CrossRef]

28.　Guerra, E.M.; Mulato, M. Synthesis and characterization of vanadium oxide/hexadecylamine membrane and its application as pH-EGFET sensor. *J. Sol-Gel Sci. Technol.* **2009**, *52*, 315–320. [CrossRef]

29.　Zulkefle, M.A.; Rahman, R.A.; Rusop, M.; Abdullah, W.F.H.; Herman, S.H. Porous TiO_2 thin film for EGFET pH sensing application. *Int. J. Eng. Technol.* **2018**, *7*, 112–114.

30.　Li, J.Y.; Chang, S.P.; Chang, S.J.; Tsai, T.Y. Sensitivity of EGFET pH sensors with TiO_2 nanowires. *ECS Solid State Lett.* **2014**, *3*, P123–P126. [CrossRef]